Science of the Total Environment 908 (2024) 168267

Contents lists available at ScienceDirect

Science of the Total Environment

journal homepage: www.elsevier.com/locate/scitotenv

Bioenergetic effects of pristine and ultraviolet-weathered polydisperse polyethylene terephthalate and polystyrene nanoplastics on human intestinal Caco-2 cells

Miao Peng [a,b,*], Maaike Vercauteren [a,b], Charlotte Grootaert [c], Ana Isabel Catarino [d], Gert Everaert [d], Andreja Rajkovic [c], Colin Janssen [a,b], Jana Asselman [a,b]

[a] Laboratory of Environmental Toxicology and Aquatic Ecology, Faculty of Bioscience Engineering, Ghent University, Coupure Links 653, 9000 Ghent, Belgium
[b] Blue Growth Research Lab, Ghent University, Wetenschapspark 1, 8400 Ostend, Belgium
[c] Department of Food Technology, Safety and Health, Faculty of Bioscience Engineering, Ghent University, Coupure Links 653, 9000 Ghent, Belgium
[d] Ocean and Human Health Division, Flanders Marine Institute, Jacobsenstraat 1, B-8400 Ostend, Belgium

HIGHLIGHTS

- Polydisperse nanoPET caused significant stimulation on bioenergetics at low concentrations (10^2-10^6 particles/mL).
- Spherical nanoPS only induced elevated glycolytic functions at the highest concentration (10^6 particles/mL).
- UV weathering could alleviate bioenergetic stress from nanoplastics and even shift the metabolic phenotype to glycolysis.

GRAPHICAL ABSTRACT

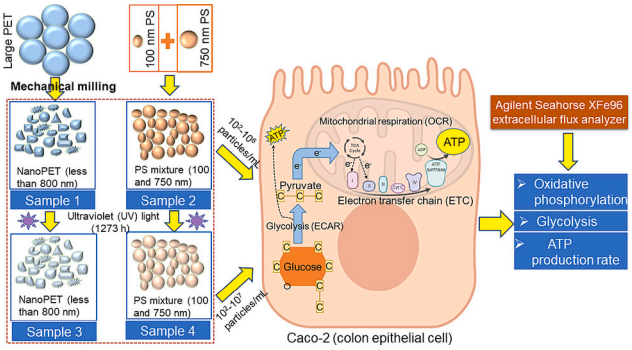

ARTICLE INFO

Editor: Lingyan Zhu

Keywords:
Nanoplastics
UV-weathering
Mitochondrial respiration
Glycolysis

ABSTRACT

The ubiquitous human exposure to nanoplastics (NPs) increasingly raises concerns regarding impact on our health. However, little is known on the biological effects of complex mixtures of weathered NPs with heterogenous size and irregular shape present in the environment. In this study, the bioenergetic effects of four such NPs mixtures on human intestinal Caco-2 cells were investigated. To this aim, Caco-2 cells were exposed to polydisperse nanoPET (<800 nm) and nanoPS (mixture of 100 and 750 nm) samples with and without ultraviolet (UV) weathering at low concentration range (10^2–10^7 particles/mL) for 48 h. Mitochondrial respiration, glycolytic functions and ATP production rates of exposed cells were measured by Seahorse XFe96 Analyzer. Among four NPs samples, polydisperse nanoPET with irregular shapes induced significant stimulation of mitochondrial respiration, glycolysis and ATP production rates in Caco-2 cells. Spherical nanoPS caused significant stimulation on glycolytic functions of Caco-2 cells at the highest concentration used (10^6 particles/mL). ATR-FTIR spectra and carbonyl index indicated formation of carbonyl groups in nanoPET and nanoPS after UV weathering. UV weathering could alleviate bioenergetic stress caused by NPs in Caco-2 cells and even shifted the

* Corresponding author at: Faculty of Bioscience Engineering, Ghent University, Coupure Links 653, 9000 Ghent, Belgium.
E-mail address: miao.peng@ugent.be (M. Peng).

https://doi.org/10.1016/j.scitotenv.2023.168267
Received 25 July 2023; Received in revised form 6 October 2023; Accepted 30 October 2023
Available online 1 November 2023

energy pathways from mitochondrial respiration to glycolysis due to electrostatic repulsion between negatively charged UV-aged NPs and cell membranes. This research is the first to study in-vitro bioenergetic responses of NPs samples with multidimensional features (polymer type, irregular shape, heterogenous size, UV-weathering) on human health. It highlights that effects between pristine and weathered NPs are different at a bioenergetic level, which has important implications for the risk assessment of NPs on human health.

1. Introduction

The increasing amounts of reports of micro- (1 μm-5 mm) and nanoplastics (<1000 nm) in human blood (Leslie et al., 2022), lung tissue (Amato-Lourenço et al., 2021), placentas (Ragusa et al., 2021) and feces (Zhang et al., 2021) raise concern on potential human health effects of plastic particles exposure. In particular, nanoplastics (NPs) are likely to pose higher health risks because they possess higher capability to cross biological barriers and have fortified surface reactivity (Cai et al., 2021b; Gigault et al., 2021; Lehner et al., 2019). For instance, it was observed that polystyrene NPs (PSNPs) could be internalized in A549 and Caco-2 cells by phagocytosis and macropinocytosis and smaller PSNPs (<100 nm) could enter into cells by clathrin- and caveolae-mediated endocytosis (Xu et al., 2021; Zhang et al., 2022). Up to date, numerous studies have assessed toxicological effects of NPs via the exposure to human cells lines (Table S1 in supporting information), which demonstrated that NPs (mainly used PS nanoparticles) induced toxic effects on cells at rather high concentrations (mostly ranging between 10^8 and 10^{12} particles/mL).

Yet, most of these reported studies made use of pristine and single-size PS spheres in vitro studies for hazard characterization, mostly to avoid dosimetry issues with sinking or floating behavior of other plastic materials, and to exclude size- and shape-related side effects. In these settings, it was observed that PS nanospheres induced toxic effects at higher concentrations. However, NPs in the real exposure environment are complex, including the presence of multiple polymer types with diverse shapes and wide size range (Alimi et al., 2022; Cai et al., 2021b). More importantly, most NPs suffer from photodegradation, chemical oxidation, hydrolysis, mechanical stress and biodegradation in the natural environment prior to human exposure (Cai et al., 2018; Sarno et al., 2021). Among them, ultraviolet (UV)-photodegradation, a major weathering pathway, changes the physicochemical characteristics of NPs such as morphology, particle size, microstructure and surface properties (Chamas et al., 2020). Moreover, UV radiation can initiate autocatalytic oxidation and induce the formation of oxygen-containing functional groups (carboxylates, hydroxyl groups, ketones or esters) potentially changing their toxicological profiles (Müller et al., 2018). Thus, it is essential to assess the biological effects of environmental NPs samples possessing multidimensionality of plastic characteristics (polymer types, shapes, size and chemical cocktail) on human health to help us reveal the toxicity of NPs sample in natural environment.

Among the NPs exposure pathways in human body, the gut is the main organ that comes into contact with these particles via ingestion (Lehner et al., 2019). The Caco-2 cell line, a human intestinal epithelial model, is commonly used to assess toxicity and metabolic homeostasis as it features many in vivo intestinal characteristics (Chen et al., 2022; Sambuy et al., 2005; Vissenaekens et al., 2021). Mitochondria play a vital role in cellular bioenergetics, redox homeostasis and regulation of apoptosis through aerobic mitochondrial respiration that produces cellular adenosine triphosphate (ATP) by oxidative phosphorylation (Kramer et al., 2014; Marchi et al., 2014; Smith et al., 2012). Glycolysis is another basic metabolic pathway to produce ATP occurring in anaerobic conditions (Kramer et al., 2014). It is reported that PS-induced oxidative stress caused significant effects on mitochondrial and glycolytic functions, as well as metabolic shift in human cell lines (Caco-2, HL-7702, L02, BEAS-2B and CCD-18Co) at high concentrations (Abdallah et al., 2022; Bonanomi et al., 2022; Halimu et al., 2022; Hu and Palić, 2020; Lin et al., 2022; R. Shen et al., 2022; Wang et al., 2022). However, the bioenergetic effects of environmental NPs as multidimensional contaminants on human health are still largely unknown.

To fill into the above research gaps, this study explored the bioenergetic effects of four simulated environmental NPs samples on human intestinal Caco-2 cells. To this aim, larger polyethylene terephthalate (PET) particles were mechanically milled into nano-size PET particles (nanoPET) with irregular shapes and heterogenous size. Then the nano-PET particles and a polystyrene nanospheres (nanoPS) mixture (100 and 750 nm) were subjected to weathering procedures. After physicochemical characterization, Caco-2 cells were exposed to nanoPET and nanoPS samples with and without UV weathering at understudied lower dose-range exposure levels (10^2–10^7 particles/mL) for 48 h. The purpose of spherical PS mixture used in this study is to benchmark our results to single-size PS nanospheres in previously published work and compare pristine versus weathered NPs in terms of effects. Polydisperse PET was tested to further explore effects of multidimensionality of plastic characteristics on human cells. The mitochondrial respiration, glycolytic functions and ATP production rates of exposed cells were measured by a Seahorse XFe96 Analyzer, to obtain crucial insights into bioenergetic responses of environmental NPs samples on human cell lines. This work integrates effects of both weathered and pristine NPs, which has important implications for the hazard characterization of NPs on human health.

2. Materials and methods

2.1. Cell culture

The adenocarcinomic human epithelial colon cell line (Caco-2) was purchased from the American Type Culture Collection (ATCC, Manassas, VA, USA) and kept under Biobank number BB190156. Caco-2 cells were grown in Dulbecco's modified eagle medium (DMEM) with addition of phenol red, 100 U/mL penicillin, 100 μg/mL streptomycin, 10 % fetal bovine serum (FBS) and 2 % nonessential amino acids (NEAA). All culture and supplemented solutions were obtained from Thermo Fisher Scientific, USA. Caco-2 cells were cultured in an incubator under 5 % CO_2, 37 °C and a relative humidity of 95 % to 100 %, and their growth and confluence were checked daily by light microscopy. Confluent cells were detached by 0.5 % Trypsin-EDTA (Thermo Fisher Scientific, USA) once a week with splitting ratio of 1:4. Caco-2 cells used in this work had the passage numbers less than value of 50.

2.2. Nanoplastic samples preparation

The preparation of four nanoplastics samples was depicted in Fig. 1. In detail, larger polyethylene terephthalate (PET) particles (IK Industrievereinigung Kunststoffverpackungen e.V., Germany) were mechanically milled into a lower size range sample (M-PET) with irregular shapes and heterogenous size by a SPEX Freezer Mill 6870 with full stainless steel milling chamber and impactors (detailed parameters setting and procedures were reported in Seghers et al., 2023). Then the M-PET was dissolved in deionized water and sonicated for 5 min. The obtained PET suspension was filtered by 0.8-μm cellulose filter to gain a sample with size <800 nm (denoted as nanoPET, sample 1). The 100-nm and 750-nm polystyrene (PS) nanospheres were obtained from Polysciences Inc. with stock solutions of 4.55×10^{13} and 1.08×10^{11} particles/mL (P/mL), respectively. After an ultrasonic treatment (5 min) and vortexing (30 s), the two nanoPS samples were mixed together and

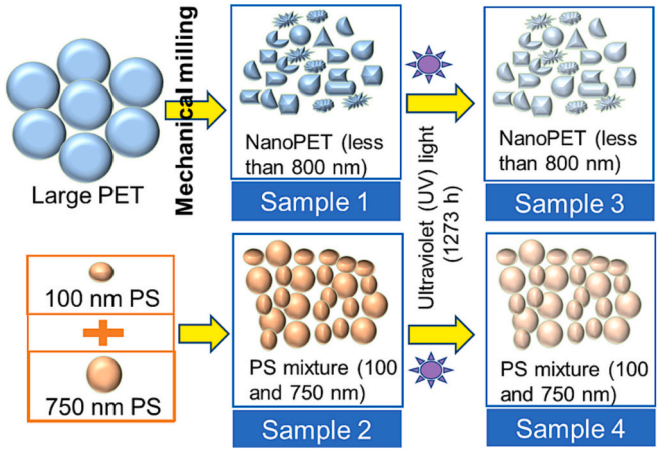

Fig. 1. The schematic overview of the nanoplastics preparation in this study.

diluted 1000 and 10 times respectively to get a mixture with particles concentration of 10^{10} P/mL, which was denoted as nanoPS (sample 2). In order to simulate photodegradation, following standard ISO guidelines, nanoPS and M-PET suspension were irradiated by ultraviolet (UV) A + B light with the emission wavelength at 300–400 nm as this range of UV light is not absorbed by ozone layer and accounts for >95 % of UV radiation that arrive to the surface of Earth (Orazio et al., 2013). The UV exposure was implemented by an Atlas Suntest CPS+ instrument fitted with a Xenon lamp (1500 W) and daylight filter with irradiation intensity of 60 W/m^2 and chamber temperature of 35 ± 3 °C. The UV irradiation time lasted for 1273 h, corresponding to 15 months of central European solar irradiance exposure (see calculation details in Supplementary file 2 of supporting information). After irradiation, the UV-weathered PET was filtered by 0.8-μm filter to get sample with size <800 nm (denoted as UV-nanoPET, sample 3). Meanwhile the UV-weathered PS was named UV-nanoPS (sample 4).

2.3. Chemical characterization of nanoplastics samples

The milled PET and UV-weathered PET suspensions were filtered over 0.8-μm filter through a glass filter system. Following the same procedure, PS and UV-weathered PS suspensions were filtered by 20-nm filter. Then the four filters were dried at room temperature for at least 24 h in a dust-free environment. Subsequently, the dried filters were measured by Fourier transform infrared spectroscopy (FTIR) (Nicolet iN10, Thermo Fisher Scientific, Madison, Wi, USA) equipped with an attenuated total-reflection diamond crystal accessory (ATR) (Nicolet iZ10, Thermo Fisher Scientific, Madison, Wi, USA). Each filter was put on the diamond stage inversely and the spectra were collected in absorbance mode from 16 scans at resolution of 4 cm^{-1}. After that, the spectra of samples were corrected by advanced ATR (diamond crystal, angle of incidence of 45, bounce number of 1.5 and sample refractive index of 1.50). The obtained spectra (.SPA files) were analyzed via OMNIC™ Anywhere and processed by Origin 9.0. Due to technical limitations, it is supposed that the changes observed in the PET particles (>800 nm) will also occur in smaller particles (<800 nm) and FTIR spectra of PET particles (>800 nm) can represent changes in nanoPET (<800 nm) to some degree in this study (see detailed explanation in Supplementary file 3). The characterization of morphology, shape, size distribution and concentration of above four nanoplastic samples was described in Supplementary file 3 of supporting information (Figs. S2–S5).

2.4. Bioenergetic profiles of Caco-2 cells

Caco-2 cells (80 μL and 8000 cells per well) were seeded in Seahorse 96-well XF Cell Culture microplates (Agilent Seahorse Bioscience, Sana Clara, CA, USA). After 48-h culture and attachment, cells were exposed to the above four nanoplastic samples with different concentrations (10^2 to 10^7 P/mL) for 48 h. Prior to the XF assay, the Seahorse XF Sensor Cartridge was loaded 180 μL of Seahorse XF Calibrant Solution. Then the hydrated cartridge was deposited at 37 °C without CO_2 for 12 h according to the manufacturer's instructions. Before the analysis, Caco-2 cells were washed twice by XF Assay Medium (Agilent Seahorse Bioscience, Sana Clara, CA, USA) with addition of 1 mM pyruvate, 10 mM glucose and 2 mM glutamine. The washed cells were kept in an incubator without CO_2 at 37 °C for 45 min. Then Caco-2 cells were treated by Agilent Seahorse Cell Mito Stress Test via a sequential injection of oligomycin (OM) (1 μM), Carbonyl cyanide-4-(trifluoromethoxy) phenylhydrazone (FCCP) (0.5 μM) and a mixture of rotenone and antimycin A (ROT/AA) (0.5 μM). Next, extracellular acidification rate (ECAR) and oxygen consumption rate (OCR) were measured by the Agilent Seahorse XFe96 extracellular flux analyzer (Agilent Seahorse Bioscience, Sana Clara, CA, USA) according to the manufacturer's instructions. The calculation process of mitochondrial respiration parameters, glycolytic parameters and ATP production rate is described in supporting information in detail (see Supplementary file 4).

2.5. Statistical analysis

All of the data in this study were normalized by the negative control (=100 %). One-way analysis of variance (ANOVA) or non-parametric Kruskal-Wallis test with Tukey post hoc test was used to perform statistical analysis via R-studio. Statistical significance was indicated as *p ≤ 0.05.

3. Results

3.1. Characterization of nanoplastics samples

The structure and functional groups of pristine and UV-weathered nanoplastics were analyzed by ATR-FTIR spectroscopy. For pristine and UV-weathered nanoPET, the characteristic absorption peaks were depicted in Fig. S1A. The spectra of UV-weathered nanoPET were the same as that of pristine nanoPET sample. Carbonyl index (CI) of PET, reflecting the degree of aging of the plastics, was calculated by the ratio of the absorbance of carbonyl groups at 1713 cm^{-1} to the absorbance of unalterable band at 721 cm^{-1} (Bai et al., 2022; P. Liu et al., 2019; Song et al., 2017). The CI values of pristine PET and UV-weathered PET are 2.38 and 2.68, respectively. The characteristic absorption peaks and corresponding wavelengths of nanoPS and UV-weathered nanoPS were displayed in Fig. S1B. Compared to virgin nanoPS, UV-weathered nanoPS had a new absorption peak at ~1715 cm^{-1} (C═O and O-C=O stretching), which is related to the presence of carboxyl groups.

3.2. Bioenergetic effects of four nanoplastics samples on Caco-2 cells

The effects on the mitochondrial respiration (oxidative phosphorylation (OXPHOS)), glycolysis and ATP production rate after 48-h exposure with varying doses of nanoplastic samples were measured by the Seahorse XF Cell Mito Stress Test kit. Overall, from Table 1, we observed no significant inhibition on three biogenetic endpoints in any treatment. In contrast, significant stimulation of certain mitochondrial and glycolytic parameters as well as ATP production rates were observed for particular set of experimental conditions, which will be reported in detail in the next sections.

3.2.1. The effects of pristine nanoPET on Caco-2 cells

The key parameters of electron transfer chain (ETC) of mitochondrial respiration were measured by sequential addition of oligomycin, FCCP and rotenone/antimycin A. As shown in Fig. 2A and B, globally, nanoPET did not cause inhibition of mitochondrial respiration at all tested

Table 1
The overview of bioenergetic effects of four nanoplastic samples on Caco-2 cells.

Endpoints	Pristine nanoPET	Pristine nanoPS	UV-weathered nanoPET	UV-weathered nanoPS
Oxidative phosphorylation	OCR ↑	0	0	0
Glycolysis	ECAR ↑	ECAR ↑	ECAR ↑	0
ATP production rate	mitoATP ↑	0	glycoATP ↑	0

Note: OCR, ECAR, mitoATP, glycoATP refer to oxygen consumption rate, extracellular acidification rate, ATP production rate from mitochondrial respiration and ATP production rate from glycolysis, respectively. The green arrows indicate significant increase induced by at least one concentration of nanoplastics.

concentrations of nanoPET. On the contrary, basal respiration (Fig. 2C) and ATP-linked respiration (Fig. 2D) showed a similar concentration-response pattern. They were significantly stimulated when Caco-2 cells were exposed to a low dose (10^3 P/mL) (about 13 % higher than the negative control, $p < 0.05$) and two highest concentrations (around 20 % higher than the negative control, $p < 0.05$). But a decrease was observed at the middle concentration (10^4 P/mL), which we could not explain based on current knowledge.

The basal glycolysis, glycolytic capacity and glycolytic reserve of nanoPET-treated Caco-2 cells after sequential injection of glucose and oligomycin are showed in Fig. 3. As depicted in Fig. 3C, only the glycolytic capacity was significantly increased when Caco-2 cells were exposed to the highest nanoPET (10^6 P/mL) (20 % higher than negative control, $p = 0.02$).

Furthermore, the ATP production rates produced from mitochondrial respiration (OXPHOS) and glycolysis were calculated through OCR and ECAR values measured by the Mito Stress kit. As shown in Fig. 4A, ATP production derived from mitochondrial respiration (mitoATP) was dominant (>80 %) in the total ATP production. In Fig. 4B, mitoATP was significantly elevated when Caco-2 cell were exposed to two highest concentrations (around 20 % higher than the negative control, $p < 0.05$), which is similar to what was observed in ATP-linked OCR (Fig. 2D). However, the glycolytic ATP production rate did not show significant response at any tested nanoPET concentration (see Fig. S6).

3.2.2. The effects of pristine nanoPS on Caco-2 cells

As shown in Fig. S7, all tested nanoPS concentrations did not induce statistically significant effects on mitochondrial respiration of Caco-2 cells. Conversely, the glycolytic functions (Fig. 5) were pointedly stimulated when Caco-2 cells were exposed to the highest nanoPS (10^6 P/mL), which was reflected in increased basal glycolysis, glycolytic capacity and glycolytic reserve that were 39 % ($p = 0.02$, Fig. 5B), 33 % ($p = 0.02$, Fig. 5C) and 28 % higher ($p = 0.009$, Fig. 5D) than the negative control, respectively. Similar to ATP production in Caco-2 cells treated with nanoPET, the ATP production rate of nanoPS-treated Caco-2 cells stemmed mainly from mitochondrial respiration (>80 %, Fig. S8A). It was observed that none of nanoPS concentrations induced statistically significant effects on mitoATP and glycoATP production rates (Fig. S8B and C).

3.2.3. The effects of UV-weathered nanoPET on Caco-2 cells

After UV weathering, none of UV-nanoPET doses led to significant effects on mitochondrial respiration (see Fig. S9). Nevertheless, as depicted in Fig. 6, glycolysis was significantly affected. In detail, basal glycolysis, glycolytic capacity, and glycolytic reserve showed concentration-dependent increasing trend from 10^2 to 10^4 P/mL, and then they decreased at two higher concentrations (10^5 and 10^6 P/mL). However, three glycolytic parameters were significantly increased at the highest dose (10^7 P/mL).

Compared to percentage of ATP production rate in Caco-2 cells exposed to pristine PET (>80 % in Fig. 4A), mitoATP production still made major contribution to total ATP production but had lower percentage (>70 %, Fig. S10A), and it was not significantly affected by any tested UV-nanoPET (Fig. S10B). Instead, glycoATP production rate, the minor contributor, was about 40 % higher than the negative control when Caco-2 cells were exposed to 10^4 and 10^7 P/mL ($p < 0.05$ for both doses, Fig. S10C).

3.2.4. The effects of UV-weathered nanoPS on Caco-2 cells

As depicted in Figs. S11 and S12, UV-weathered nanoPS did not evoke any significant effects on mitochondrial respiration, glycolytic functions, and ATP production rate under all tested concentrations.

4. Discussion

This study is to the best of our knowledge the first one to compare the metabolic phenotypes of an established intestinal cell line exposed to two types of nanoplastics using a realistic low dose approach and UV weathering as key experimental variables. Despite observed ranges of observed biological responses, which is inherent to the complex experimental setup and low dose approach, notable effects on metabolic pathways were found showing differences among types of nanoplastics, tested concentrations and weathering conditions. As depicted in Fig. 2E, mitochondrial respiration (oxidative phosphorylation) and glycolysis are two vital energy pathways in cellular bioenergetics, and they produce adenosine triphosphate (ATP) by aerobic and anaerobic ways, respectively. Thus, three endpoints (mitochondrial respiration, glycolysis and ATP production rate) could be considered as early markers of cell dysfunctionality which may lead to chronic disorders. Indeed, recent papers (Jeong and Choi, 2019; Rubio et al., 2020) have demonstrated that oxidative stress is potentially one of the key mechanisms by which nanoplastics affect cells. Mitochondria are regarded as initiator and the first target of oxidative stress, and can be impaired due to the internalization of nanoplastics in cells (Bonanomi et al., 2022; Lin et al., 2022). Moreover, it has been reported that nanoplastics can directly interact with and be internalized in mitochondria, leading to mitochondrial stress and PINK1/Parkin-mediated mitophagy (Xu et al., 2023). The stress by nanoplastics is likely to perturb cellular metabolism (energy pathways or energy production rate) as well.

In our study, the first observation is that none of the four tested NPs inhibited mitochondrial respiration, glycolysis and ATP production rate, thereby indicating a lack of cytotoxicity under applied experimental conditions. This important finding is in line with expectations based on low dose approach and confirms some of the previous studies (F. Shen et al., 2022; Xu et al., 2021). In contrast to the expectations our results have shown that some of the low dose conditions (10^2–10^7 P/mL) have stimulated cellular metabolism of Caco-2 cells at different endpoints. Also, some studies reported significant inhibition on glycolysis at extremely high concentration of 100 μg/mL (3.55×10^{11} P/mL, PS, 80 nm) (Wang et al., 2022) as well as on mitochondrial respiration at 40 μg/mL (9.08×10^{12} P/mL, PS, 20 nm) (Halimu et al., 2022). This hormesis effect is a dose-response phenomenon characterized by low-dose stimulation and high-dose inhibition. Although improved ATP production is in general seen as positive signal, especially when it comes from mitochondrial respiration, the determination of whether the hormesis based stimulation is beneficial or not should be decoupled from a decision as to whether the response is hormetic or not. It is important to note that exposure time as well as extended time of observation of a given endpoint may result in different outcomes and no assumptions on positive effects of low dose exposure to nanoplastics should be made, instead the hormetic stimulation should be seen as an effect of fundamental reparative processes of the cell in response to an onset of the disruption of homeostasis (Calabrese et al., 2015).

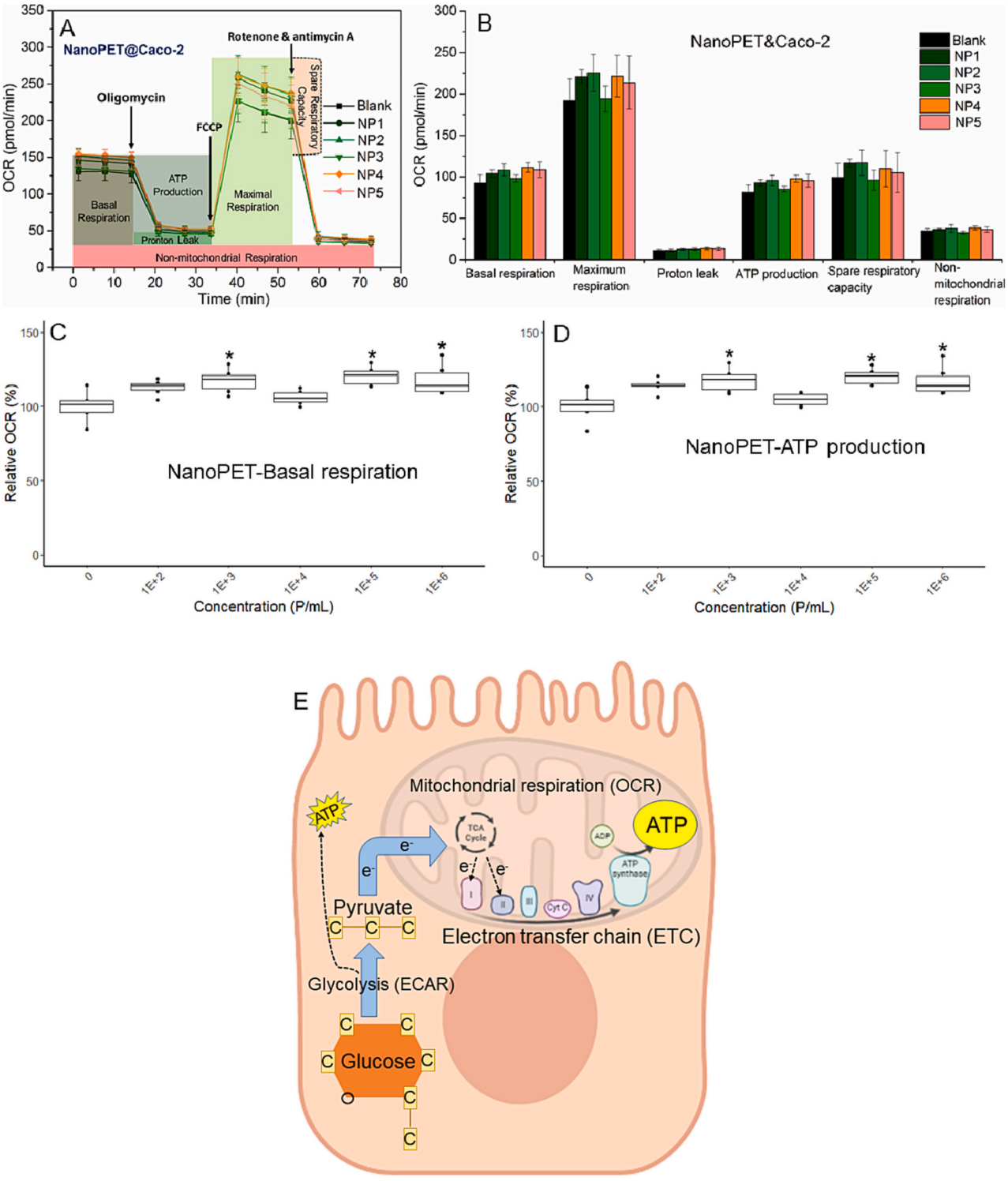

Fig. 2. Effects of pristine nanoPET on mitochondrial respiration of Caco-2 cells after 48-h exposure. (A) Mitochondrial profiles of nanoPET-treated Caco-2 in response to sequential administration of pharmacological modulators of the mitochondrial electron transport chain. (B) Mitochondrial parameters of Caco-2 cells by measuring oxygen consumption rate (OCR). Relative OCR from basal respiration (C) and ATP production (D) in Caco-2 cells. (E) Metabolic pathways (mitochondrial respiration and glycolysis) in Caco-2 cells. n = 6; *p ≤ 0.05, significant difference from negative control. (NP1-NP5 correspond to nanoPET concentrations of 10^2, 10^3, 10^4, 10^5 and 10^6 P/mL, respectively.)

A second observation is that when comparing pristine nanoPET with nanoPS, we could observe an increased glycolytic response for both samples, but the mitochondrial parameters were only significantly increased in nanoPET-treated Caco-2 cells. Indeed, significantly elevated basal respiration and ATP-linked respiration indicate that mitochondria need to consume more oxygen and produce more ATP, possibly to counteract cellular stress from nanoPET exposure. The significant increase on the ATP production rates derived from mitochondrial respiration (mitoATP) confirmed the stimulated effects on oxidative phosphorylation. Nevertheless, glycolytic functions were more tolerant to nanoPET. Only the glycolytic capacity, representing the maximum glycolytic rate, showed an increase at the highest nanoPET

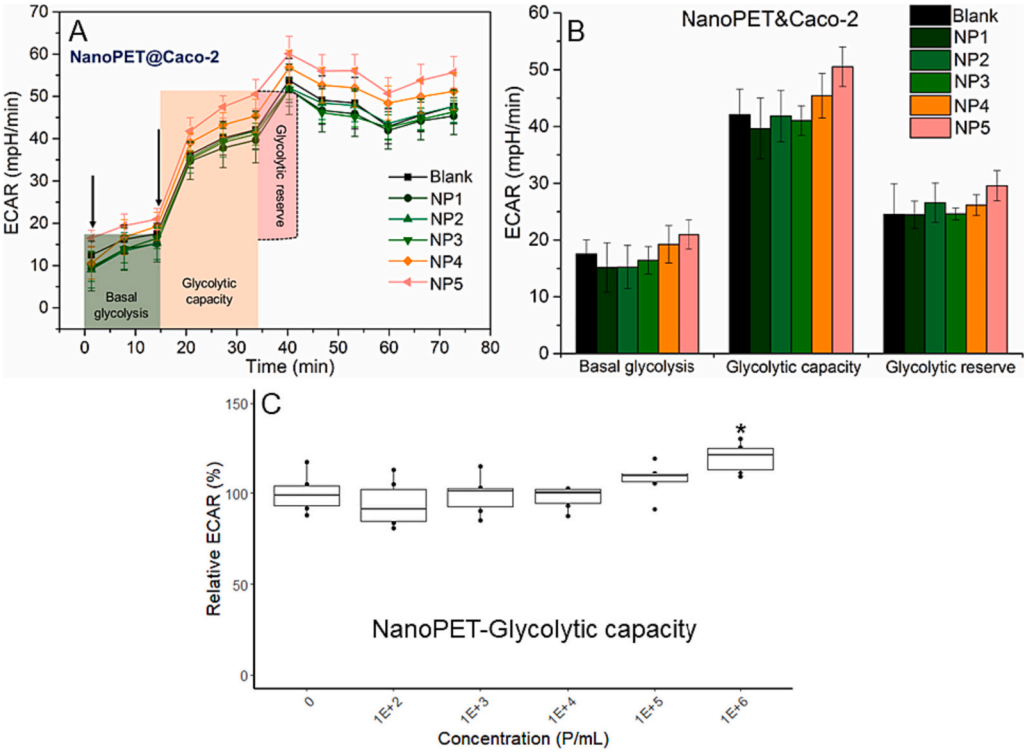

Fig. 3. Effects of pristine nanoPET on glycolysis of Caco-2 cells after 48-h exposure. (A) Glycolytic profiles of nanoPET-treated Caco-2 in response to sequential administration of pharmacological modulators of glycolysis. (B) Glycolytic parameters of Caco-2 cells by measuring extracellular acidification rate (ECAR). (C) Relative ECAR from glycolytic capacity in Caco-2 cells. n = 6; *p ≤ 0.05, significant difference from negative control. (NP1-NP5 correspond to nanoPET concentrations of 10^2, 10^3, 10^4, 10^5 and 10^6 P/mL, respectively.)

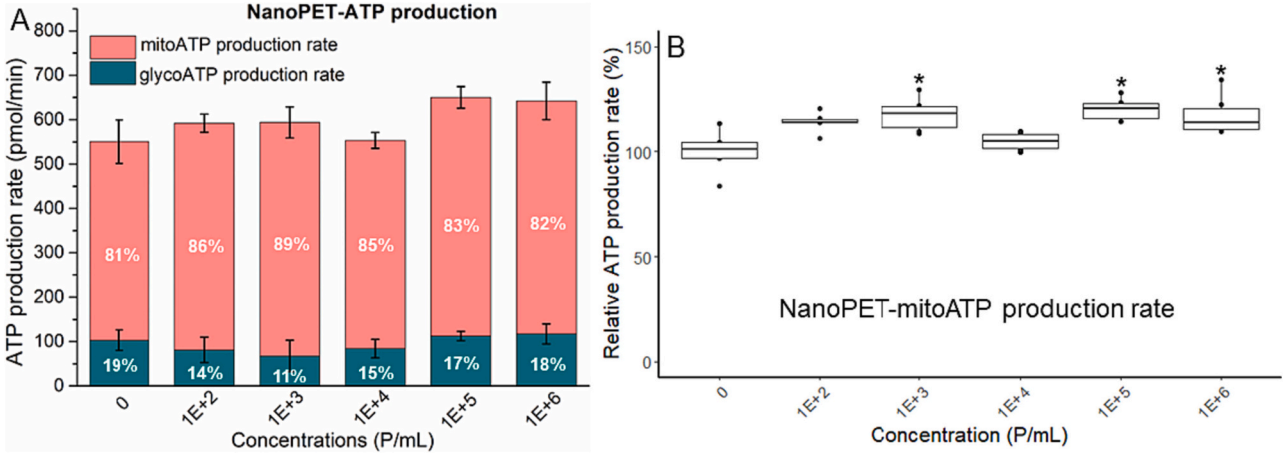

Fig. 4. (A) Effects of pristine nanoPET on mitochondrial and glycolytic ATP production rates in Caco-2 cells after 48 h exposure. (B) Relative mitochondrial ATP production rate (mitoATP) in Caco-2 cell. Absolute ATP production rates were normalized by the negative control (set as 100 %). n = 6; *p ≤ 0.05, significant difference from negative control.

concentration (10^6 P/mL). On the contrary, glycolytic performance was more sensitive to nanoPS sample than that mitochondrial functions. Only stress from the highest dose (10^6 P/mL) was high enough to significantly stimulate ECAR on three glycolytic parameters (basal glycolysis, glycolytic capacity and reserve). The metabolic difference between nanoPET (irregular shapes) and nanoPS (spheres) can be attributed to 1) polymer type, 2) size distribution and 3) particle shape and morphology. Here, polymer type, particle shape and morphology seem to be most likely to contribute the most to effects. Indeed, with regards to the size distribution, the nanoPS contained both the smallest and largest particle size also present in the nanoPET. Hence, different metabolism due to size is likely not the cause. In contrast, particle shape and morphology may influence corona formation and interaction with proteins and cell membrane receptors (Martin et al., 2022). Moreover, a study found nanoPET with lower hydrophobicity, compared to nanoPS, can easily penetrate cell membrane due to fewer absorbed lipids via molecular dynamics simulation (Li et al., 2023). Similarly, some studies reported that uptake mechanisms depended on physicochemical properties such as polymer type, particle size and hydrophobicity (da Silva Brito et al., 2023; Liu et al., 2021), but the used nanoplastics are monodisperse spheres. Another research work reported that irregular microplastics (polyethylene (PE)) particles with sharp edge and higher

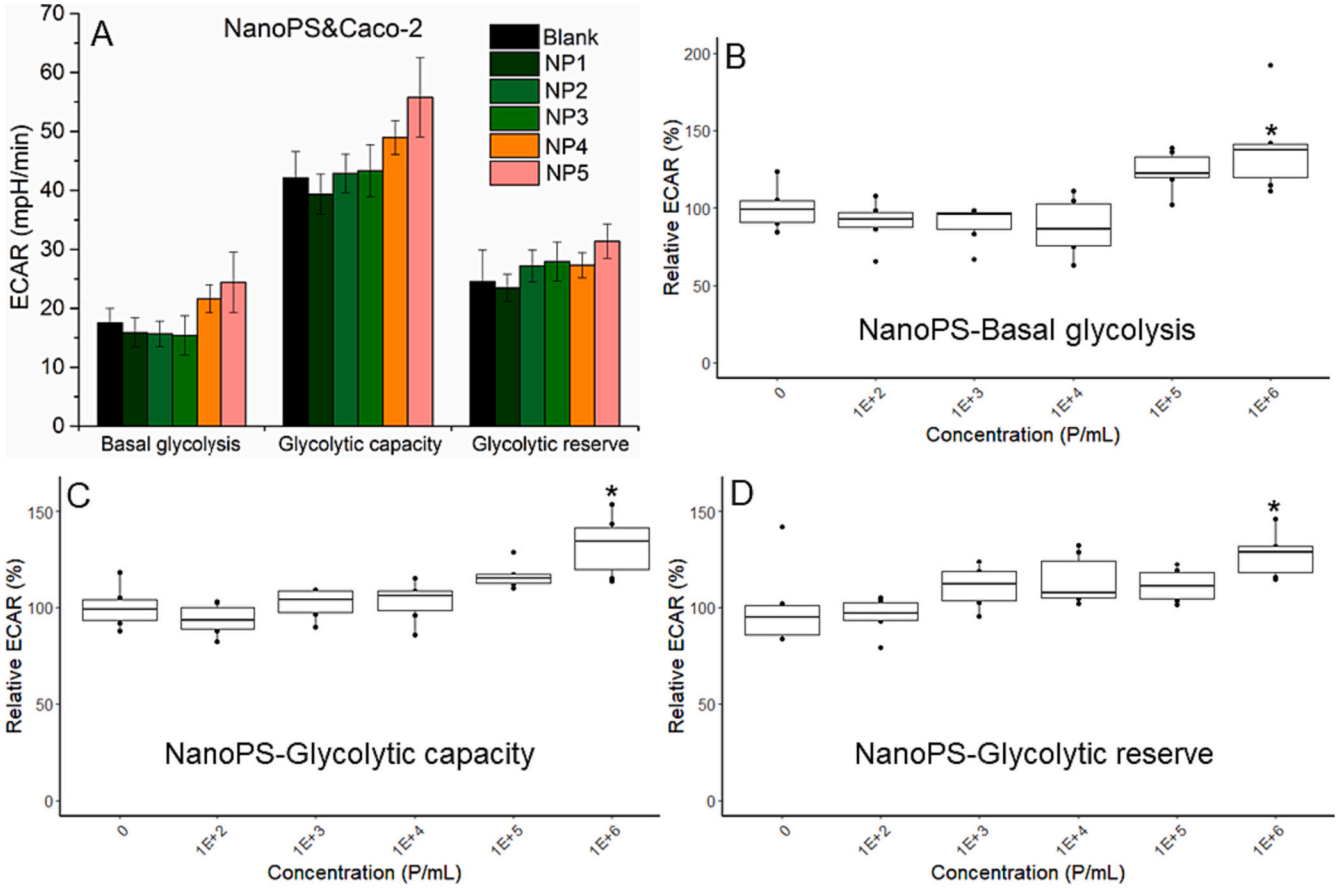

Fig. 5. Effects of pristine nanoPS on glycolysis of Caco-2 cells after 48 h exposure. (A) Glycolytic parameters of Caco-2 cells by measuring extracellular acidification rate (ECAR). Relative ECAR from basal glycolysis (B), glycolytic capacity (C) and glycolytic reserve (D) in Caco-2 cells. n = 6; *p ≤ 0.05, significant difference from negative control. (NP1-NP5 correspond to nanoPS concentrations of 10^2, 10^3, 10^4, 10^5 and 10^6 P/mL, respectively.)

curvature change were more toxic than spherical PE beads with smooth surface morphology (Choi et al., 2021), which could be extrapolated to nanoplastics.

To our best knowledge, there are only a few scientific papers that reported effects of nanoplastics (predominant nanoPS) on bioenergetics of human cells. Among these publications, significant inhibition of glycolysis was observed at extremely high concentration of 100 μg/mL (3.55×10^{11} P/mL, PS, 80 nm) (Wang et al., 2022). Similarly, one study observed mitochondrial stimulation at 10 μg/mL (2.27×10^{12} P/mL, PS, 20 nm) and inhibition at 40 μg/mL (9.08×10^{12} P/mL, PS, 20 nm) (Halimu et al., 2022). Another study reported inhibited mitochondrial respiration at concentration of 250 μg/mL (8.75×10^{11} P/mL, PS, 80 nm) (Lin et al., 2022). The absence of inhibition in our study is attributed to lower concentrations used here (10^2–10^7 P/mL), i.e. 10^3–10^5 times lower than the previous work, that represent realistic exposure concentrations based on the current knowledge (Cai et al., 2021a; Cai et al., 2021b; Hernandez et al., 2019; Sullivan et al., 2020) (Table S2). Compared to monodisperse nanoPS used in the above publications, nanoPS mixture (100 and 750 nm) implemented in this study did not cause effects on mitochondrial respiration, which further indicates that particle concentration could be a more important factor than particle size. Also, our study is the first to show that particle characteristics influence the bioenergetic effects of human cells, underlining the need to test different particles in terms of shape, size and polymer type.

A third observation is that the UV weathering affected the surface properties of NPs and thus UV-weathered NPs resulted in different bioenergetic effects compared to pristine counterparts. Due to the intrinsic C═O stretch of carboxylic group in PET, it is difficult to measure spectra changes before and after UV weathering. However, UV-weathered PET with higher CI demonstrated that more carboxylic acid groups were induced by strong degree of photo-oxidation from UV irradiation. Our results are in line with other published studies (Bai et al., 2022; Beltrán-Sanahuja et al., 2020). Compared to pristine nanoPS, a new oxygen-containing group (-COOH) was observed for aged nanoPS after UV weathering. This indicates that the UV-nanoPS particles have a negative surface charge in comparison to the pre-weathered particles. This surface change was reported in other publications as well (Shi et al., 2021; Yu et al., 2022). In addition, despite insignificant morphological change on nanoPS before and after UV weathering, the particle size of UV-nanoPS was slightly smaller than pristine nanoPS. Similarly, the size distribution of UV-nanoPET shifted to a lower range with the smaller mean size compared to virgin nanoPET. This decrease in nanoplastic size has been reported by previous studies as well (Y. Liu et al., 2019; Shi et al., 2021).

Reports have indicated that micro-/nanoplastics could cross cell membranes and be accumulated in cells (Cortés et al., 2020; Xu et al., 2021) as well as change morphology of cells (Goodman et al., 2021). Furthermore, it is found that nanoPS can directly interact with mitochondrial membranes and was internalized in mitochondria at 2.18×10^{11} P/mL, leading to mitochondrial stress in Caco-2 cells (Xu et al., 2023). Previous studies demonstrated that nanoPS with positive charge were more readily internalized in cell lines and induced more damage to cells than counterparts with negative charge and without charge due to electrostatic attraction directed to negatively charged cell membrane (Abdallah et al., 2022; Kloet et al., 2015; Li et al., 2022; Paget et al., 2015; Ruenraroengsak and Tetley, 2015). However, some studies reported that UV-aged nanoPS particles with carboxylic group exerted greater cytotoxicity than pristine nanoPS owing to intrinsic toxicity or

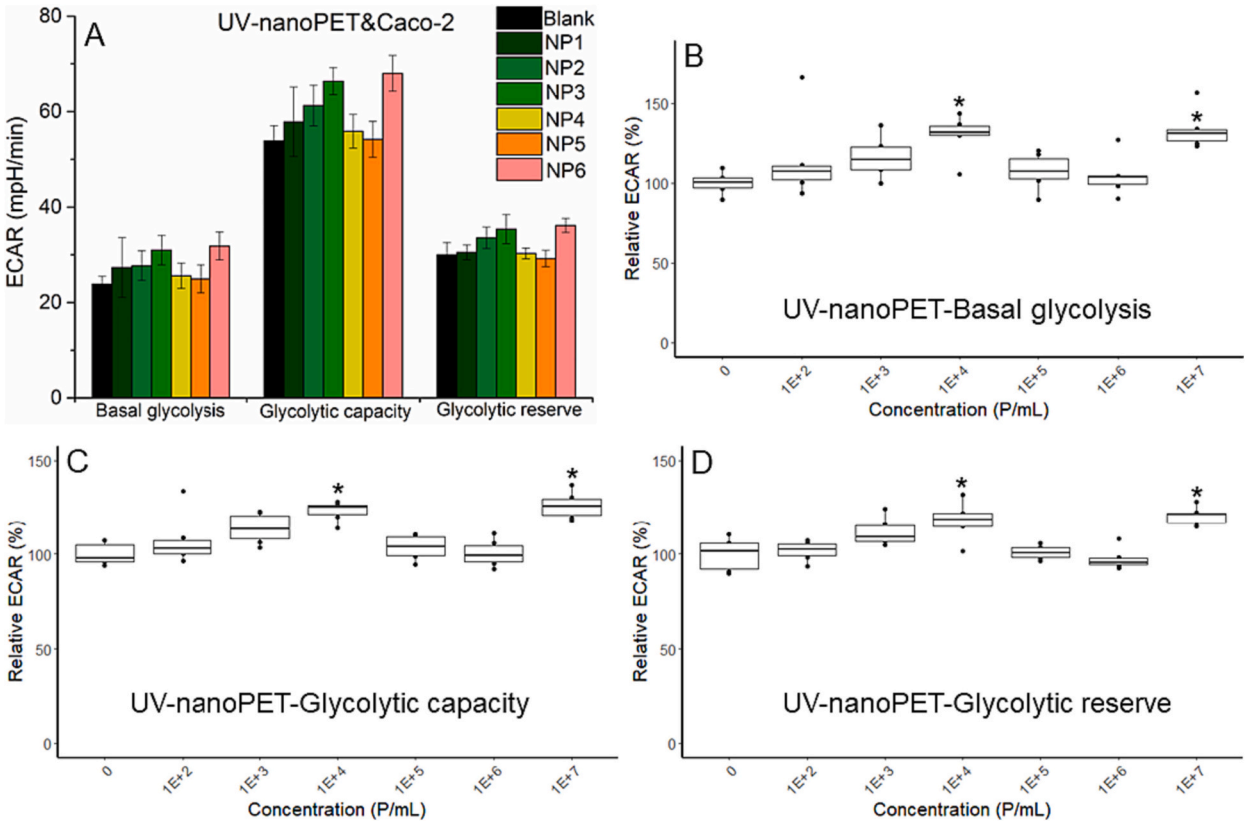

Fig. 6. Effects of UV-nanoPET on glycolysis of Caco-2 cells after 48 h exposure. (A) Glycolytic parameters of Caco-2 cells by measuring extracellular acidification rate (ECAR). Relative ECAR from basal glycolysis (B), glycolytic capacity (C) and glycolytic reserve (D) in Caco-2 cells. n = 6; *p ≤ 0.05, significant difference from negative control. (NP1-NP6 correspond to nanoPS concentrations of 10^2, 10^3, 10^4, 10^5, 10^6 and 10^7 P/mL, respectively.)

bioactivity of functional groups (specific interaction with biomolecules such as oligonucleotides, antibodies or other proteins) in cells at rather high concentrations (10^8–10^{10} P/mL) (Shi et al., 2021; Yu et al., 2022). In this study, after UV weathering, different from pristine nanoPET, significant bioenegetic effects shifted from mitochondrial respiration to anaerobic energy pathway where UV-nanoPET displayed elevated glycolytic functions and glycolytic ATP production rate at the intermediate and the highest concentrations. Our results support the general consensus that electrostatic repulsion between negatively charged UV-nanoPET (with carboxylic group) and cell membranes as well as mitochondrial membranes could reduce efficiency of cellular uptake and further decrease mitochondrial bioavailable UV-nanoPET compared to virgin nanoPET. Thus there would be much less UV-nanoPET particles that interact with mitochondria and no significant effects on mitochondrial functions were observed in Caco-2 cells exposed to UV-nanoPET. Instead, the retained UV-nanoPET in cells could induce significant effects on glycolysis occurring in cytoplasm. Similarly, due to electrostatic repulsion, negatively charged UV-weathered PS particles could be less internalized in cell membrane and hardly interact with mitochondria, and thus UV-nanoPS did not cause effects on mitochondrial respiration. However differences across all these studies could be attributed to different characteristics (polymer type, size distribution and morphology) between UV-weathered and pristine nanoplastics. Therefore, instead of arbitrarily concluding that aged nanoplastics possess higher or lower cytotoxicity, we need to consider potentially involved factors (concentration and physicochemical properties) to provide a more nuanced assessment of their impact on cellular health. Based on the above elucidation, this work demonstrates that UV-weathering could alleviate bioenergetic stress caused by NPs in Caco-2 cells and even shift energy pathway from mitochondrial respiration to glycolysis.

This study reveals that energy metabolism of Caco-2 cells could be stimulated or shifted from aerobic to anaerobic pathways under the exposure to NPs samples with multidimensional characteristics (polymer type, irregular shape, heterogenous size, UV-weathering) at low concentrations. However, it has some limitations and perspectives: 1) NPs generally coexist with other contaminants (such as heavy metals, dissolved organic matters and persistent organic pollutants) in complicated matrices (Bhagat et al., 2021; Okoye et al., 2022; Yu et al., 2019). Thus co-effects on cellular energy metabolism should be tested in the future studies; 2) different bioenergetic effects induced by nanoPET and nanoPS are attributed to their physicochemical discrepancies (polymer types, size distribution and particle shapes as well as morphology) in this study. Therefore, more detailed studies should be explored to distinguish the roles of these physicochemical properties in cellular bioenergetics; 3) prior to exposure to colon cells, ingested NPs would be weathered by saliva, gastric fluid and intestinal fluid. As such, it is essential to test toxicity of nanoplastics with multiple artificial weathering processes.

5. Conclusions

In this study, Caco-2 cells were exposed to four simulated environmental NPs samples (nanoPET, nanoPS, UV-nanoPET and UV-nanoPS) at low concentrations (10^2–10^7 particles/mL). Mitochondrial respiration and ATP production rate from oxidative phosphorylation were stimulated by exposure to pristine nanoPET while anaerobic glycolysis and glycolytic ATP production rate were enhanced under exposure of UV-weathered nanoPET. Glycolytic functions were stimulated when Caco-2 cells were exposed to high virgin nanoPS dose, however, UV-weathered nanoPS did not cause any significant effect on metabolic phenotypes of Caco-2 cells. This study is the first to investigate

metabolic phenotypes of Caco-2 cells exposed to NPs samples with multidimensional features (polymer type, irregular shape, heterogenous size, UV-weathering) at low concentrations. It highlights that effects between virgin and weathered nanoplastics are different at a bio-energetic level.

CRediT authorship contribution statement

Miao Peng: Conceptualization, Methodology, Writing - Original draft preparation, Funding acquisition. **Maaike Vercauteren:** Writing - Review & editing, Funding acquisition. **Charlotte Grootaert:** Formal analysis, Methodology, Writing - Review & editing. **Ana Isabel Catarino:** Writing - Review & editing, Methodology. **Gert Everaert:** Writing - Review & editing, Methodology. **Andreja Rajkovic:** Writing - Review & editing, Funding acquisition. **Colin Janssen:** Supervision. **Jana Asselman:** Writing - Review & editing, Supervision.

Declaration of competing interest

The authors declare that they have no known competing financial interests or personal relationships that could have appeared to influence the work reported in this paper.

Data availability

Data will be made available on request.

Acknowledgements

Miao Peng is a PhD student financially supported by China Scholarship Council (CSC) (File No. 201906150135) and UGent special research fund (BOFCHN2019000801). Maaike Vercauteren is funded by the BOF-research grant (grant code BOF21/PDO/081). We express our gratitude to Ghent University's Special Research Fund for their generous support in acquiring the Seahorse equipment (BOF.BAS.2020.0035.01). This research was partially supported by the ImpTox project, funded under the European Union's Horizon 2020 - Research and Innovation Framework Programme with grant No. 965173. We extend our gratitude to the Centre for Advanced Light Microscopy at Ghent University (Belgium) for their valuable support and access to confocal microscopy resources as well.

Appendix A. Supplementary data

Supplementary data to this article can be found online at https://doi.org/10.1016/j.scitotenv.2023.168267.

References

Abdallah, M.F., Muda, E.V.S., Grootaert, C., Rajkovic, A., 2022. Subtoxic Doses of Polystyrene Nanoplastics and Microcystin-LR Affect the Bioenergetic Status of Caco-2 and HepG2 Cells, pp. S307–S308.

Alimi, O.S., Claveau-Mallet, D., Kurusu, R.S., Lapointe, M., Bayen, S., Tufenkji, N., 2022. Weathering pathways and protocols for environmentally relevant microplastics and nanoplastics: what are we missing? J. Hazard. Mater. 423, 126955.

Amato-Lourenço, L.F., Carvalho-Oliveira, R., Júnior, G.R., dos Santos Galvão, L., Ando, R.A., Mauad, T., 2021. Presence of airborne microplastics in human lung tissue. J. Hazard. Mater. 416, 126124.

Bai, X., Li, F., Ma, L., Li, C., 2022. Weathering of geotextiles under ultraviolet exposure: a neglected source of microfibers from coastal reclamation. Sci. Total Environ. 804, 150168.

Beltrán-Sanahuja, A., Casado-Coy, N., Simó-Cabrera, L., Sanz-Lázaro, C., 2020. Monitoring polymer degradation under different conditions in the marine environment. Environ. Pollut. 259, 113836.

Bhagat, J., Nishimura, N., Shimada, Y., 2021. Toxicological interactions of microplastics/nanoplastics and environmental contaminants: current knowledge and future perspectives. J. Hazard. Mater. 405, 123913.

Bonanomi, M., Salmistraro, N., Porro, D., Pinsino, A., Colangelo, A.M., Gaglio, D., 2022. Polystyrene micro and nano-particles induce metabolic rewiring in normal human colon cells: a risk factor for human health. Chemosphere 303, 134947.

Cai, L., Wang, J., Peng, J., Wu, Z., Tan, X., 2018. Observation of the degradation of three types of plastic pellets exposed to UV irradiation in three different environments. Sci. Total Environ. 628-629, 740–747.

Cai, H., Chen, M., Du, F., Matthews, S., Shi, H., 2021a. Separation and enrichment of nanoplastics in environmental water samples via ultracentrifugation. Water Res. 203, 117509.

Cai, H., Xu, E.G., Du, F., Li, R., Liu, J., Shi, H., 2021b. Analysis of environmental nanoplastics: progress and challenges. Chem. Eng. J. 410, 128208.

Calabrese, E.J., Dhawan, G., Kapoor, R., Iavicoli, I., Calabrese, V., 2015. HORMESIS: a fundamental concept with widespread biological and biomedical applications. Gerontology 62 (5), 530–535.

Chamas, A., Moon, H., Zheng, J., Qiu, Y., Tabassum, T., Jang, J.H., Abu-Omar, M., Scott, S.L., Suh, S., 2020. Degradation rates of plastics in the environment. ACS Sustain. Chem. Eng. 8 (9), 3494–3511.

Chen, X., Abdallah, M.F., Grootaert, C., Rajkovic, A., 2022. Bioenergetic status of the intestinal and hepatic cells after short term exposure to fumonisin B1 and aflatoxin B1. Int. J. Mol. Sci. 23 (13), 6945.

Choi, D., Hwang, J., Bang, J., Han, S., Kim, T., Oh, Y., Hwang, Y., Choi, J., Hong, J., 2021. In vitro toxicity from a physical perspective of polyethylene microplastics based on statistical curvature change analysis. Sci. Total Environ. 752, 142242.

Cortés, C., Domenech, J., Salazar, M., Pastor, S., Marcos, R., Hernández, A., 2020. Nanoplastics as a potential environmental health factor: effects of polystyrene nanoparticles on human intestinal epithelial Caco-2 cells. Environ. Sci. Nano 7 (1), 272–285.

da Silva Brito, W.A., Singer, D., Miebach, L., Saadati, F., Wende, K., Schmidt, A., Bekeschus, S., 2023. Comprehensive in vitro polymer type, concentration, and size correlation analysis to microplastic toxicity and inflammation. Sci. Total Environ. 854, 158731.

Gigault, J., El Hadri, H., Nguyen, B., Grassl, B., Rowenczyk, L., Tufenkji, N., Feng, S., Wiesner, M., 2021. Nanoplastics are neither microplastics nor engineered nanoparticles. Nat. Nanotechnol. 16 (5), 501–507.

Goodman, K.E., Hare, J.T., Khamis, Z.I., Hua, T., Sang, Q.-X.A., 2021. Exposure of human lung cells to polystyrene microplastics significantly retards cell proliferation and triggers morphological changes. Chem. Res. Toxicol. 34 (4), 1069–1081.

Halimu, G., Zhang, Q., Liu, L., Zhang, Z., Wang, X., Gu, W., Zhang, B., Dai, Y., Zhang, H., Zhang, C., Xu, M., 2022. Toxic effects of nanoplastics with different sizes and surface charges on epithelial-to-mesenchymal transition in A549 cells and the potential toxicological mechanism. J. Hazard. Mater. 430, 128485.

Hernandez, L.M., Xu, E.G., Larsson, H.C.E., Tahara, R., Maisuria, V.B., Tufenkji, N., 2019. Plastic teabags release billions of microparticles and nanoparticles into tea. Environ. Sci. Technol. 53 (21), 12300–12310.

Hu, M., Palić, D., 2020. Micro- and nano-plastics activation of oxidative and inflammatory adverse outcome pathways. Redox Biol. 37, 101620.

Jeong, J., Choi, J., 2019. Adverse outcome pathways potentially related to hazard identification of microplastics based on toxicity mechanisms. Chemosphere 231, 249–255.

Kloet, S.K., Walczak, A.P., Louisse, J., van den Berg, H.H.J., Bouwmeester, H., Tromp, P., Fokkink, R.G., Rietjens, I.M.C.M., 2015. Translocation of positively and negatively charged polystyrene nanoparticles in an in vitro placental model. Toxicol. in Vitro 29 (7), 1701–1710.

Kramer, P.A., Ravi, S., Chacko, B., Johnson, M.S., Darley-Usmar, V.M., 2014. A review of the mitochondrial and glycolytic metabolism in human platelets and leukocytes: implications for their use as bioenergetic biomarkers. Redox Biol. 2, 206–210.

Lehner, R., Weder, C., Petri-Fink, A., Rothen-Rutishauser, B., 2019. Emergence of nanoplastic in the environment and possible impact on human health. Environ. Sci. Technol. 53 (4), 1748–1765.

Leslie, H.A., van Velzen, M.J.M., Brandsma, S.H., Vethaak, A.D., Garcia-Vallejo, J.J., Lamoree, M.H., 2022. Discovery and quantification of plastic particle pollution in human blood. Environ. Int. 163, 107199.

Li, Y., Xu, M., Zhang, Z., Halimu, G., Li, Y., Li, Y., Gu, W., Zhang, B., Wang, X., 2022. In vitro study on the toxicity of nanoplastics with different charges to murine splenic lymphocytes. J. Hazard. Mater. 424, 127508.

Li, L., Li, S., Xu, Y., Ren, L., Yang, L., Liu, X., Dai, Y., Zhao, J., Yue, T., 2023. Distinguishing the nanoplastic–cell membrane interface by polymer type and aging properties: translocation, transformation and perturbation. Environ. Sci. Nano 10 (2), 440–453.

Lin, S., Zhang, H., Wang, C., Su, X.-L., Song, Y., Wu, P., Yang, Z., Wong, M.-H., Cai, Z., Zheng, C., 2022. Metabolomics reveal nanoplastic-induced mitochondrial damage in human liver and lung cells. Environ. Sci. Technol. 56 (17), 12483–12493.

Liu, P., Qian, L., Wang, H., Zhan, X., Lu, K., Gu, C., Gao, S., 2019a. New insights into the aging behavior of microplastics accelerated by advanced oxidation processes. Environ. Sci. Technol. 53 (7), 3579–3588.

Liu, Y., Hu, Y., Yang, C., Chen, C., Huang, W., Dang, Z., 2019b. Aggregation kinetics of UV irradiated nanoplastics in aquatic environments. Water Res. 163, 114870.

Liu, L., Xu, K., Zhang, B., Ye, Y., Zhang, Q., Jiang, W., 2021. Cellular internalization and release of polystyrene microplastics and nanoplastics. Sci. Total Environ. 779, 146523.

Marchi, S., Patergnani, S., Pinton, P., 2014. The endoplasmic reticulum–mitochondria connection: one touch, multiple functions. Biochim. Biophys. Acta BBA Bioenergetics 1837 (4), 461–469.

Martin, L.M.A., Gan, N., Wang, E., Merrill, M., Xu, W., 2022. Materials, surfaces, and interfacial phenomena in nanoplastics toxicology research. Environ. Pollut. 292, 118442.

Müller, A., Becker, R., Dorgerloh, U., Simon, F.-G., Braun, U., 2018. The effect of polymer aging on the uptake of fuel aromatics and ethers by microplastics. Environ. Pollut. 240, 639–646.

Okoye, C.O., Addey, C.I., Oderinde, O., Okoro, J.O., Uwamungu, J.Y., Ikechukwu, C.K., Okeke, E.S., Ejeromedoghene, O., Odii, E.C., 2022. Toxic chemicals and persistent organic pollutants associated with micro- and nanoplastics pollution. Chem. Eng. J. Adv. 11, 100310.

Orazio, J., Jarrett, S., Amaro-Ortiz, A., Scott, T., 2013. UV Radiation and the Skin, pp. 12222–12248.

Paget, V., Dekali, S., Kortulewski, T., Grall, R., Gamez, C., Blazy, K., Aguerre-Chariol, O., Chevillard, S., Braun, A., Rat, P., Lacroix, G., 2015. Specific uptake and genotoxicity induced by polystyrene nanobeads with distinct surface chemistry on human lung epithelial cells and macrophages. PLoS One 10 (4), e0123297.

Ragusa, A., Svelato, A., Santacroce, C., Catalano, P., Notarstefano, V., Carnevali, O., Papa, F., Rongioletti, M.C.A., Baiocco, F., Draghi, S., D'Amore, E., Rinaldo, D., Matta, M., Giorgini, E., 2021. Plasticenta: first evidence of microplastics in human placenta. Environ. Int. 146, 106274.

Rubio, L., Barguilla, I., Domenech, J., Marcos, R., Hernández, A., 2020. Biological effects, including oxidative stress and genotoxic damage, of polystyrene nanoparticles in different human hematopoietic cell lines. J. Hazard. Mater. 398, 122900.

Ruenraroengsak, P., Tetley, T.D., 2015. Differential bioreactivity of neutral, cationic and anionic polystyrene nanoparticles with cells from the human alveolar compartment: robust response of alveolar type 1 epithelial cells. Part. Fibre Toxicol. 12 (1), 19.

Sambuy, Y., De Angelis, I., Ranaldi, G., Scarino, M.L., Stammati, A., Zucco, F., 2005. The Caco-2 cell line as a model of the intestinal barrier: influence of cell and culture-related factors on Caco-2 cell functional characteristics. Cell Biol. Toxicol. 21 (1), 1–26.

Sarno, A., Olafsen, K., Kubowicz, S., Karimov, F., Sait, S.T.L., Sørensen, L., Booth, A.M., 2021. Accelerated hydrolysis method for producing partially degraded polyester microplastic fiber reference materials. Environ. Sci. Technol. Lett. 8 (3), 250–255.

Seghers, J., Cella, C., Pequeur, E., Spina, R., Mehn, D., Gilliland, D., Emteborg, H., 2023. Preparation of high numbers of artificially aged micro- and nano plastic particles for environmental and toxicological studies. Anal. Bioanal. Chem. (In preparation).

Shen, F., Li, D., Guo, J., Chen, J., 2022a. Mechanistic toxicity assessment of differently sized and charged polystyrene nanoparticles based on human placental cells. Water Res. 223, 118960.

Shen, R., Yang, K., Cheng, X., Guo, C., Xing, X., Sun, H., Liu, D., Liu, X., Wang, D., 2022b. Accumulation of polystyrene microplastics induces liver fibrosis by activating cGAS/STING pathway. Environ. Pollut. 300, 118986.

Shi, Q., Tang, J., Liu, X., Liu, R., 2021. Ultraviolet-induced photodegradation elevated the toxicity of polystyrene nanoplastics on human lung epithelial A549 cells. Environ. Sci. Nano 8 (9), 2660–2675.

Smith, R.A.J., Hartley, R.C., Cochemé, H.M., Murphy, M.P., 2012. Mitochondrial pharmacology. Trends Pharmacol. Sci. 33 (6), 341–352.

Song, Y.K., Hong, S.H., Jang, M., Han, G.M., Jung, S.W., Shim, W.J., 2017. Combined effects of UV exposure duration and mechanical abrasion on microplastic fragmentation by polymer type. Environ. Sci. Technol. 51 (8), 4368–4376.

Sullivan, G.L., Gallardo, J.D., Jones, E.W., Hollliman, P.J., Watson, T.M., Sarp, S., 2020. Detection of trace sub-micron (nano) plastics in water samples using pyrolysis-gas chromatography time of flight mass spectrometry (PY-GCToF). Chemosphere 249, 126179.

Vissenaekens, H., Smagghe, G., Criel, H., Grootaert, C., Raes, K., Rajkovic, A., Goeminne, G., Boon, N., De Schutter, K., Van Camp, J., 2021. Intracellular quercetin accumulation and its impact on mitochondrial dysfunction in intestinal Caco-2 cells. Food Res. Int. 145, 110430.

Wang, H., Shi, X., Gao, Y., Zhang, X., Zhao, H., Wang, L., Zhang, X., Chen, R., 2022. Polystyrene nanoplastics induce profound metabolic shift in human cells as revealed by integrated proteomic and metabolomic analysis. Environ. Int. 166, 107349.

Xu, D., Ma, Y., Han, X., Chen, Y., 2021. Systematic toxicity evaluation of polystyrene nanoplastics on mice and molecular mechanism investigation about their internalization into Caco-2 cells. J. Hazard. Mater. 417, 126092.

Xu, D., Ma, Y., Peng, C., Gan, Y., Wang, Y., Chen, Z., Han, X., Chen, Y., 2023. Differently surface-labeled polystyrene nanoplastics at an environmentally relevant concentration induced Crohn's ileitis-like features via triggering intestinal epithelial cell necroptosis. Environ. Int. 176, 107968.

Yu, F., Yang, C., Zhu, Z., Bai, X., Ma, J., 2019. Adsorption behavior of organic pollutants and metals on micro/nanoplastics in the aquatic environment. Sci. Total Environ. 694, 133643.

Yu, X., Lang, M., Huang, D., Yang, C., Ouyang, Z., Guo, X., 2022. Photo-transformation of microplastics and its toxicity to Caco-2 cells. Sci. Total Environ. 806, 150954.

Zhang, J., Wang, L., Trasande, L., Kannan, K., 2021. Occurrence of polyethylene terephthalate and polycarbonate microplastics in infant and adult feces. Environ. Sci. Technol. Lett. 8 (11), 989–994.

Zhang, Y.-X., Wang, M., Yang, L., Pan, K., Miao, A.-J., 2022. Bioaccumulation of differently-sized polystyrene nanoplastics by human lung and intestine cells. J. Hazard. Mater. 439, 129585.